

Supporting Information

Effect of Porosity Parameters and Surface Chemistry on Carbon Dioxide Adsorption in Sulfur-Doped Porous Carbons

En-Jie Wang,[†] Zhu-Yin Sui,^{*,‡} Ya-Nan Sun,[‡] Zhuang Ma,^{*,†} Bao-Hang Han^{*,‡,§}

[†] *School of Materials Science and Engineering, Liaoning Technical University, Fuxin 123000, China*

[‡] *CAS Key Laboratory of Nanosystem and Hierarchical Fabrication, CAS Center for Excellence in Nanoscience, National Center for Nanoscience and Technology, Beijing 100190, China*

[§] *University of Chinese Academy of Sciences, Beijing 100049, China*

Tel: +86 10 8254 5576. Email: hanbh@nanoctr.cn.

Tel: +86 10 8254 5708. E-mail: suizy@nanoctr.cn.

Tel: +86 244 5861 003. E-mail: mazh123@263.net.

Instrumental Characterization

The morphology was acquired from an S-4800 scanning electron microscope (Hitachi Ltd., Japan) with an energy dispersive X-ray spectrometer. X-ray diffraction pattern was collected on a Philips X’Pert PRO X-ray diffractometer (PANalytical B.V., Netherlands). Raman spectrum was obtained on an inVia Raman spectrometer (Renishaw plc, U.K.) at room temperature. XPS analysis was characterized by using an ESCALab220i-XL X-ray photoelectron spectrometer system (VG Scientific Ltd., U.K.). The elemental analysis was conducted with a Flash EA 1112 analyzer (Carlo Erba, Italy). Nitrogen adsorption–desorption measurements were conducted on a 3Flex surface characterization analyzer (Micromeritics Instrument Corporation, U.S.A.). The pore parameters such as specific surface area, pore size distribution, and pore volume were obtained based on the nitrogen sorption isotherms of the as-prepared samples at 77 K. The pore size distribution profiles were obtained according to a non-local density functional theory method. A TriStar II 3020 surface area and porosity analyzer (Micromeritics Instrument Corporation, U.S.A.) was utilized to obtain the sorption isotherms of carbon dioxide of the as-prepared SPCs. The ultramicropore volumes were calculated from carbon dioxide isotherms of the as-prepared samples at 273K by applying Dubinin–Radushkevich equation.

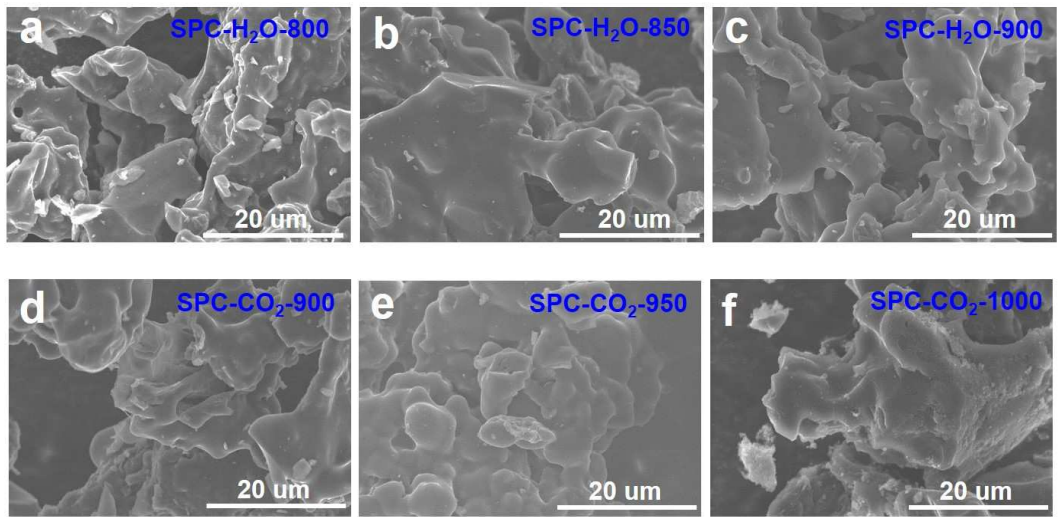


Figure S1. SEM images of (a) SPC-H₂O-800, (b) SPC-H₂O-850, (c) SPC-H₂O-900, (d) SPC-CO₂-900, (e) SPC-CO₂-950, and (f) SPC-CO₂-1000 prepared at different activation conditions.

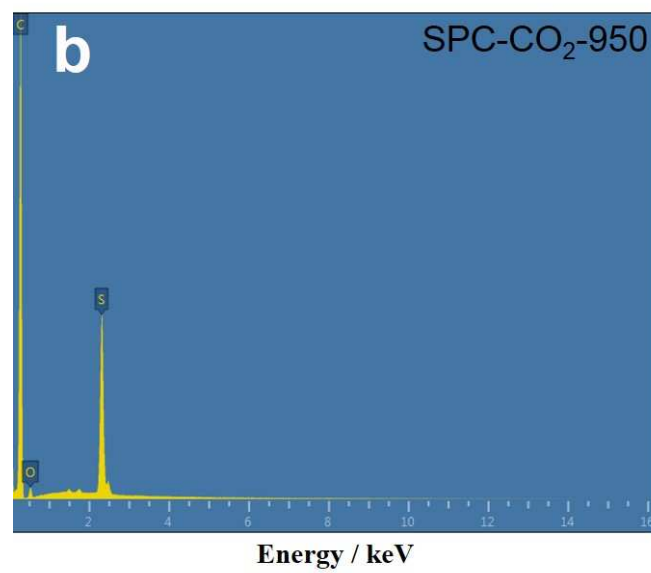
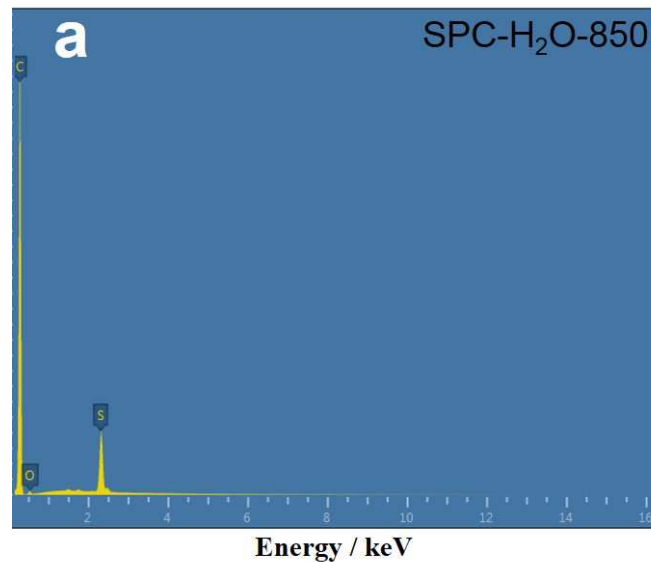


Figure S2. The energy dispersive X-ray spectra of SPC-H₂O-850 and SPC-CO₂-950.

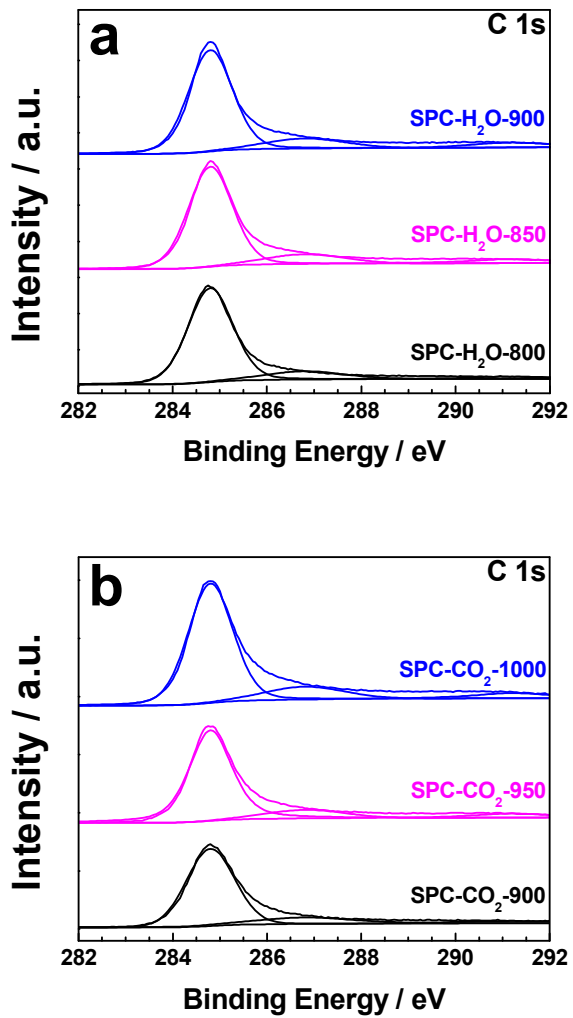


Figure S3. (a) High-resolution C 1s spectra of SPC-H₂O-800, SPC-H₂O-850, and SPC-H₂O-900; (b) high-resolution C 1s spectra of SPC-CO₂-900, SPC-CO₂-950, and SPC-CO₂-1000.

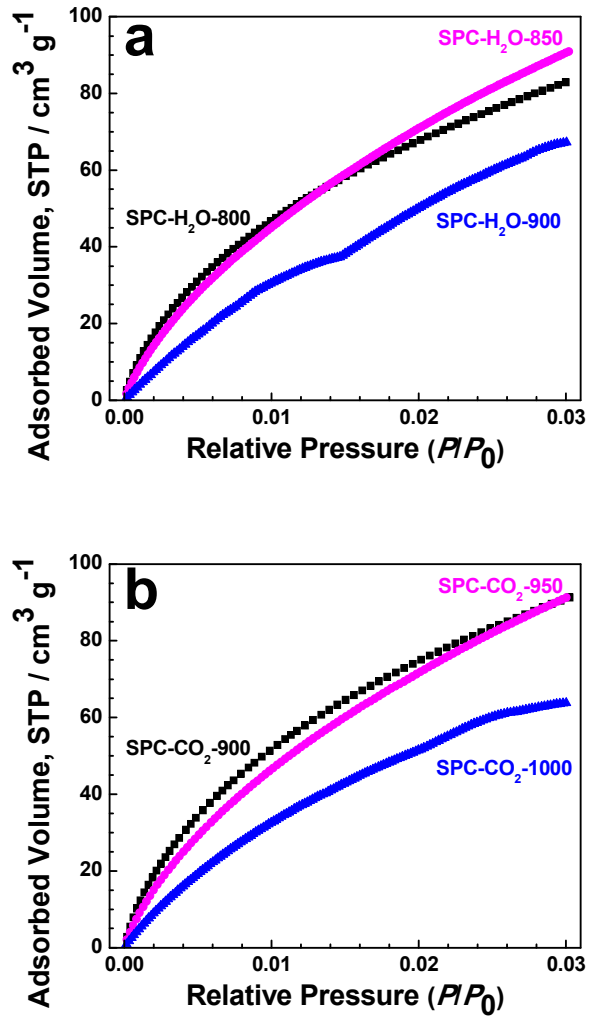


Figure S4. (a) Carbon dioxide adsorption isotherms of (a) SPC-H₂O-800, SPC-H₂O-850, and SPC-H₂O-900 at 273 K; (b) carbon dioxide adsorption isotherms of SPC-CO₂-900, SPC-CO₂-950, and SPC-CO₂-1000 at 273 K. These isotherms were used to calculate ultramicropore volumes by the Dubinin–Radushkevich method.

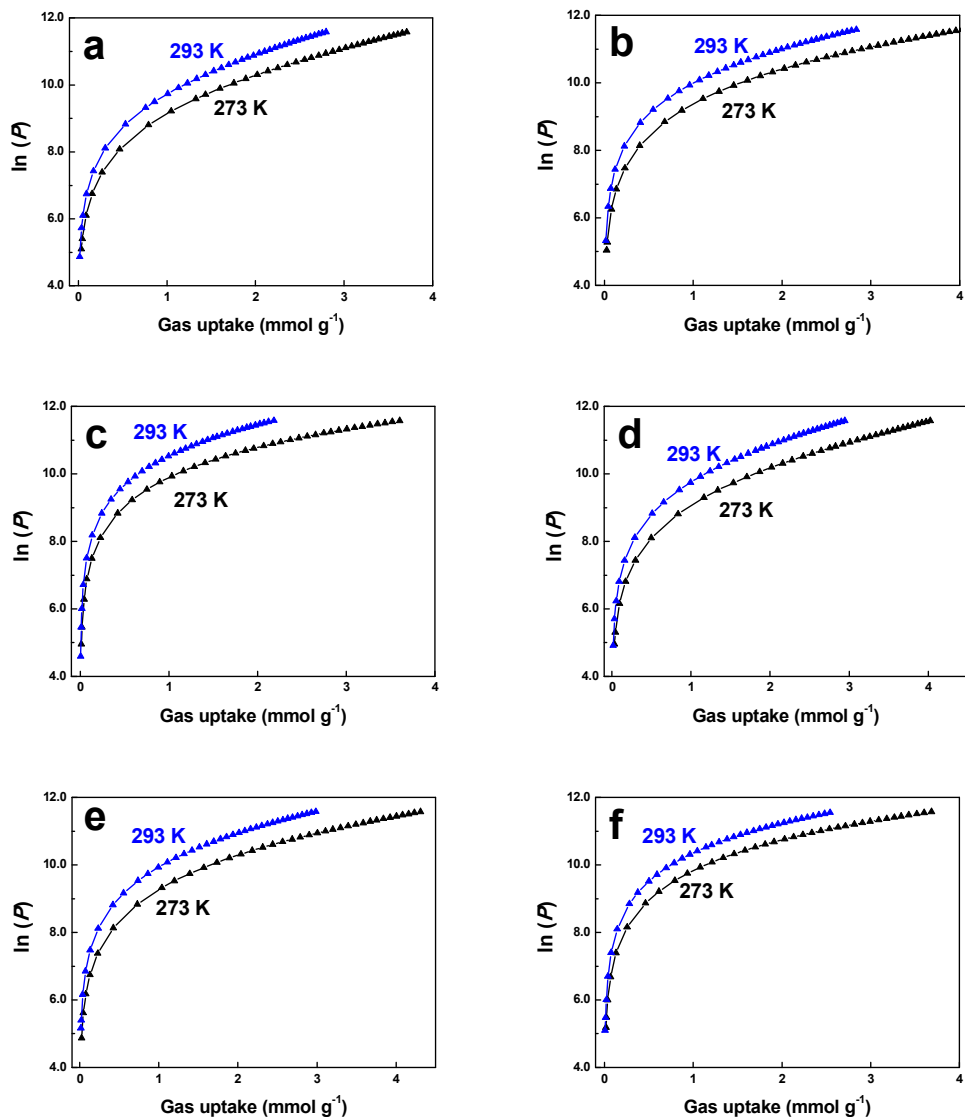


Figure S5. Virial analysis of carbon dioxide adsorption data (273 and 293 K) for (a) SPC-H₂O-800, (b) SPC-H₂O-850, (c) SPC-H₂O-900, (d) SPC-CO₂-900, (e) SPC-CO₂-950, and (f) SPC-CO₂-1000.

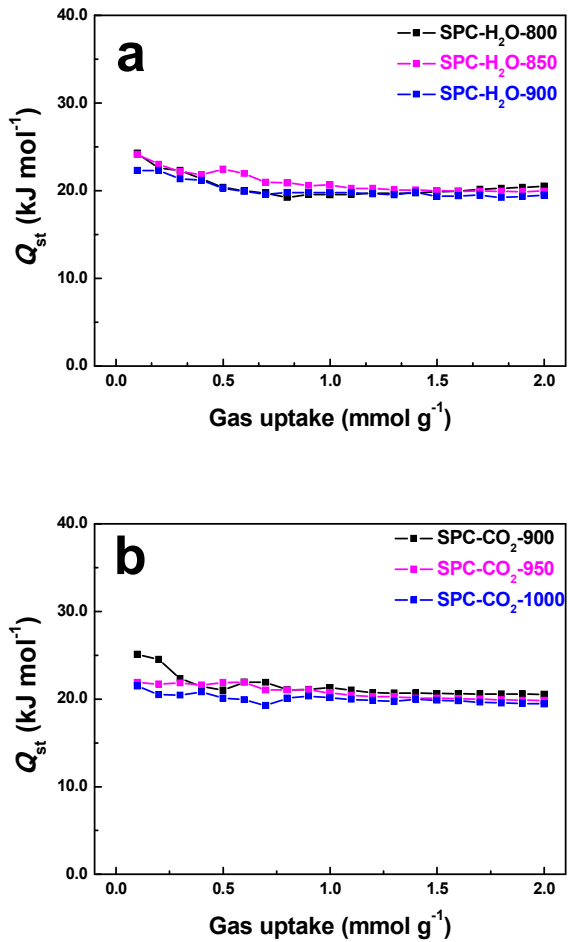


Figure S6. Q_{st} for SPC-H₂O- T (a) and SPC-CO₂- T series of samples (b) as a function of carbon dioxide adsorption amounts.

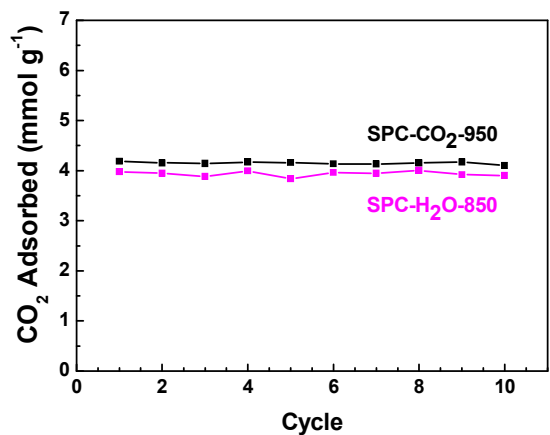


Figure S7. The cycling performance of SPC-H₂O-850 and SPC-CO₂-950 for carbon dioxide uptake.

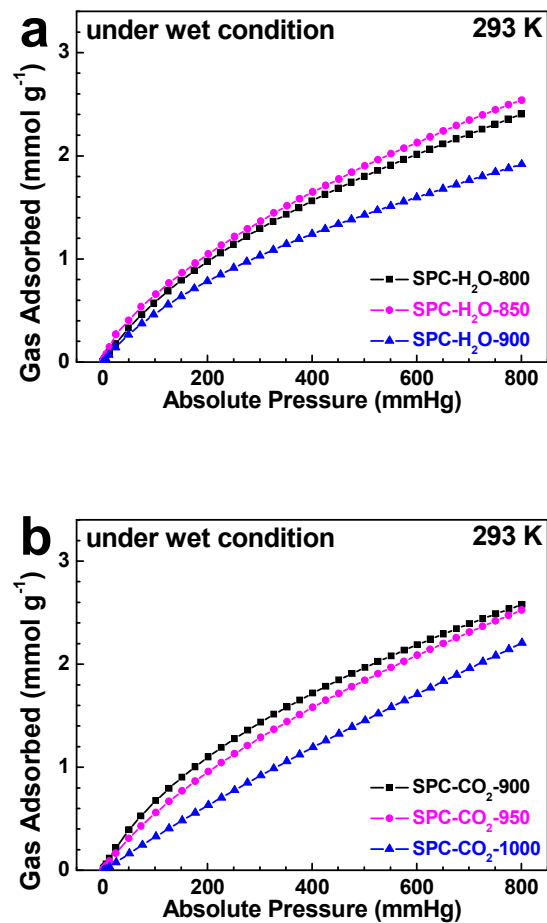


Figure S8. The carbon dioxide uptake of SPC-H₂O-*T* (a) and SPC-CO₂-*T* series of samples (b) under wet condition at 293 K.

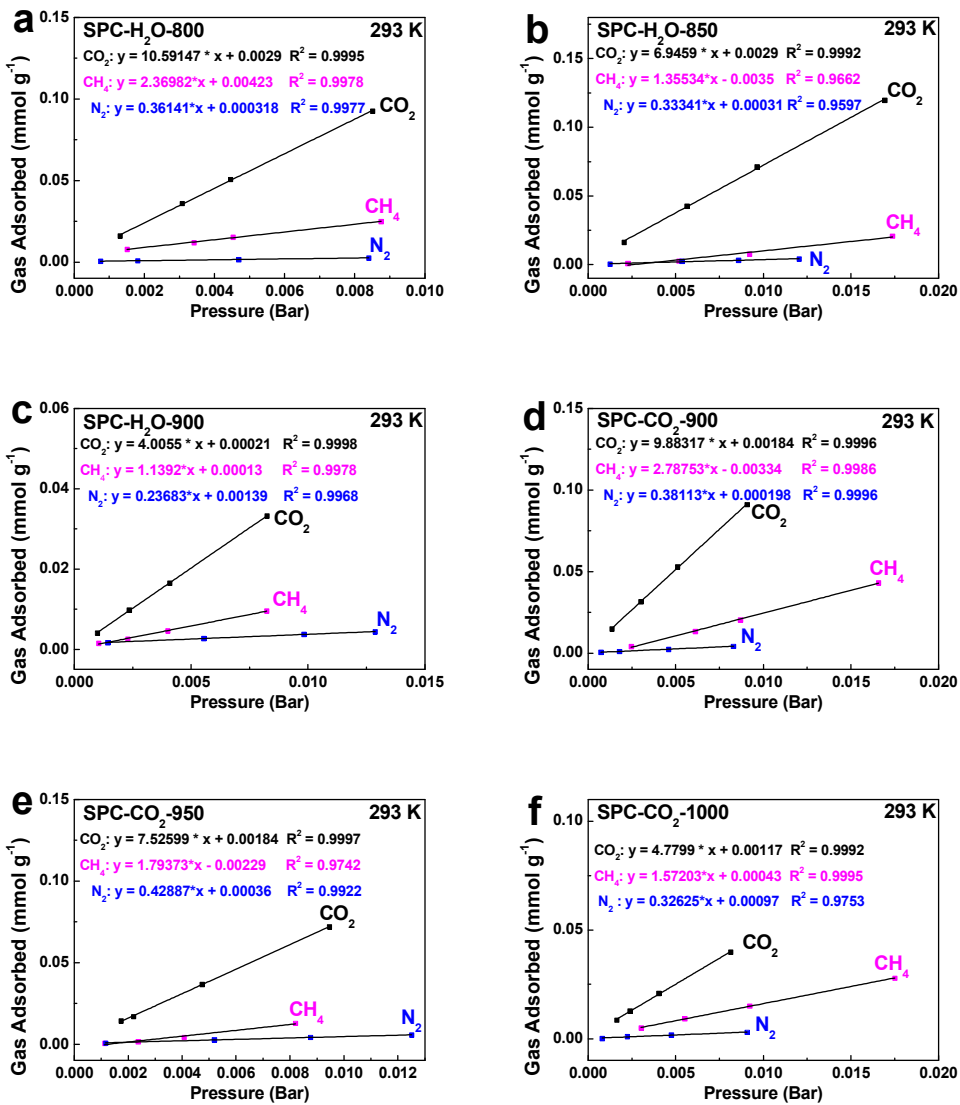


Figure S9. CO₂/CH₄ and CO₂/N₂ initial slope selectivity studies for (a) SPC-H₂O-800, (b) SPC-H₂O-850, (c) SPC-H₂O-900, (d) SPC-CO₂-900, (e) SPC-CO₂-950, and (f) SPC-CO₂-1000.

Table S1. Chemical composition for SPC-H₂O-*T* and SPC-CO₂-*T* series of samples obtained from elemental analysis and XPS.

Sample	elemental analysis (wt. %)			XPS (at. %)		
	C	S	O	C	S	O
SPC-H ₂ O-800	84.3	6.8	4.5	91.5	3.4	5.1
SPC-H ₂ O-850	86.9	3.8	6.8	92.0	1.9	6.1
SPC-H ₂ O-900	90.4	1.9	4.4	94.5	0.6	4.9
SPC-CO ₂ -900	78.3	10.3	8.5	87.4	4.9	7.7
SPC-CO ₂ -950	83.2	8.1	3.9	91.7	4.3	4.0
SPC-CO ₂ -1000	85.6	6.7	4.1	90.6	3.9	5.5

Table S2. CO₂/CH₄ and CO₂/N₂ initial slope selectivity for SPC-H₂O-800, SPC-H₂O-850, SPC-H₂O-900, SPC-CO₂-900, SPC-CO₂-950, and SPC-CO₂-1000.

Sample	CO ₂ /CH ₄ selectivity	CO ₂ /N ₂ selectivity
SPC-H ₂ O-800	4.5	29.3
SPC-H ₂ O-850	5.1	20.8
SPC-H ₂ O-900	3.5	16.9
SPC-CO ₂ -900	3.5	25.9
SPC-CO ₂ -950	4.2	17.5
SPC-CO ₂ -1000	3.0	14.7

Table S3. Carbon dioxide adsorption performance comparison of SPCs with other porous materials.

Sample	S_{BET} ($\text{m}^2 \text{ g}^{-1}$)	T	CO ₂ uptake at 0.15 bar (mmol g ⁻¹)	CO ₂ uptake at 1.0 bar (mmol g ⁻¹)	Ref.
SPC-H ₂ O-850	1110	273 K	1.19	3.89	This work
SPC-H ₂ O-850	1110	293 K	0.77	2.73	This work
SPC-CO ₂ -950	1230	273 K	1.29	4.16	This work
SPC-CO ₂ -950	1230	293 K	0.81	2.87	This work
N-doped carbon (a-NDC6)	1588	298 K	–	4.30	[S1]
conjugated microporous polymer (CMPPN-2)	1368	273 K	–	0.87	[S2]
microporous organic polymer (SPBI-1)	600	273 K	–	3.09	[S3]
graphene					
aerogel-derived porous carbon	1230	273 K	0.61	2.45	[S4]
reduced graphene oxide (HRGO-100)	530	273 K	0.97	2.40	[S5]
N-doped porous carbon (PNC-6)	2900	273 K	0.82	3.91	[S6]
S-doped microporous carbon (a-SG6)	1396	298 K	–	4.50	[S7]
porous carbon (PAC5/700)	968	298 K	0.77	–	[S8]
porous carbon (nCN2600)	979	298 K	1.0	2.8	[S9]
porous carbon (SD2600)	866	298 K	1.3	4.3	[S9]
metal–organic frameworks (Mg-MOF-74(S))	1640	298 K	5.43	7.95	[S10]

The dash (–) indicates that the value is not given in the reference.

The abbreviation in parentheses is given according to the original references.

References

- [S1] Chandra, V.; Yu, S. U.; Kim, S. H.; Yoon, Y. S.; Kim, D. Y.; Kwon, A. H.; Meyyappan, M.; Kim, K. S. Highly Selective CO₂ Capture on N-doped Carbon Produced by Chemical Activation of Polypyrrole Functionalized Graphene Sheets. *Chem. Commun.* **2012**, 48 (5), 735–737.
- [S2] Chen, Y. F.; Sun, H. X.; Yang, R. X.; Wang, T. T.; Pei, C. J.; Xiang, Z. T.; Zhu, Z. Q.; Liang, W. D.; Li, A.; Deng, W. Q. Synthesis of Conjugated Microporous Polymer Nanotubes with Large Surface Areas as Absorbents for Iodine and CO₂ Uptake. *J. Mater. Chem. A* **2015**, 3 (1), 87–91.
- [S3] Zhao, Y.-C.; Wang, T.; Zhang, L.-M.; Cui, Y.; Han, B.-H. Microporous Spiro-Centered Poly(benzimidazole) Networks: Preparation, Characterization, and Gas Sorption Properties. *Polym. Chem.* **2015**, 6 (5), 748–753.
- [S4] Sui, Z.-Y.; Meng, Q.-H.; Li, J.-T.; Zhu, J.-H.; Cui, Y.; Han, B.-H. High Surface Area Porous Carbons Produced by Steam Activation of Graphene Aerogels. *J. Mater. Chem. A* **2014**, 2 (25), 9891–9898.
- [S5] Sui, Z.-Y.; Han, B.-H. Effect of Surface Chemistry and Textural Properties on Carbon Dioxide Uptake in Hydrothermally Reduced Graphene Oxide. *Carbon* **2015**, 82, 590–598.
- [S6] Li, X.; Sui, Z.-Y.; Sun, Y.-N.; Xiao, P.-W.; Wang, X.-Y.; Han, B.-H. Polyaniline-Derived Hierarchically Porous Nitrogen-Doped Carbons as Gas Adsorbents for Carbon Dioxide Uptake. *Micropor. Mesopor. Mater.* **2018**, 257, 85–91.
- [S7] Seema, H.; Kemp, K. C.; Le, N. H.; Park, S.-W.; Chandra, V.; Lee, J. W.; Kim, K. S. Highly Selective CO₂ Capture by S-Doped Microporous Carbon Materials. *Carbon*

2014, *66*, 320–326.

[S8] Sánchez-Sánchez, Á.; Suárez-García, F.; Martínez-Alonso, A.; Tascón, J. Influence of Porous Texture and Surface Chemistry on the CO₂ Adsorption Capacity of Porous Carbons: Acidic and Basic Site Interactions. *ACS Appl. Mater. Interfaces* **2014**, *6* (23), 21237–21247.

[S9] Adeniran, B.; Mokaya, R. Is N-Doping in Porous Carbons Beneficial for CO₂ Storage? Experimental Demonstration of the Relative Effects of Pore Size and N-Doping. *Chem. Mater.* **2016**, *28* (3), 994–1001.

[S10] Yang, D.-A.; Cho, H.-Y.; Kim, J.; Yang, S.-T.; Ahn, W.-S. CO₂ Capture and Conversion using Mg-MOF-74 Prepared by a Sonochemical Method. *Energy Environ. Sci.* **2012**, *5* (4), 6465–6473.